Available online at www.eccomasproceedia.org
Eccomas Proceedia SMART (2025) 1170-1178

ECCOMAS
Proceedia

XI ECCOMAS Thematic Conference on Smart Structures and Materials - SMART 2025
M. Krommer, M. Nader and M. Schagerl (Eds)

Received: 14 April 2025 / Revised: 8 September 2025 / Accepted: 10 September 2025
© The Author(s) 2025

Multi-Frequency Adaptive Tuned Mass Dampers Through Intelligent Materials

Stefano Manzoni, Marta Berardengo, Francescantonio Lucá

Abstract. Tuned mass dampers are well-known systems used for lowering vibrations of a primary system. Although they are effective and reliable, their main drawback is related to the need of a perfect tuning between the dynamic features of the tuned mass damper and the primary system. When mistuning occurs (e.g., due to thermal shifts), the attenuation performance worsens. To solve this issue, adaptive tuned mass dampers, able to change their dynamic features and recover the tuned condition, have been proposed in the literature. One of the most promising approaches is the use of intelligent materials to make tuned mass dampers adaptive, since often this choice allows obtaining the adaptation with lightweight and simple layouts. Some examples are related to piezoelectric-based and shape memory alloy-based adaptive tuned mass dampers. This paper aims at showing how it is possible to adapt different eigenfrequencies of a tuned mass damper at the same time with a given level of independence. More in detail, it will be shown that N tuned mass damper eigenfrequencies can be adapted by using N (or more) elements of intelligent materials fixed to the primary structure and shunting them with proper electric impedances. The paper treats in detail the example of piezoelectric patches but it also underlines that other materials (e.g., magnetostrictive elements) can be used following the same logical approach and the same mathematical treatment. In the discussed case of piezoelectric elements, each of them will be shunted with a capacitance (one capacitance for each patch; each capacitance can be either positive or negative). Experiments carried out on a beam equipped with two piezoelectric patches are presented to confirm the feasibility and reliability of the proposed method.

Key words: Multi-frequency, Adaptive, Tuned mass damper, Vibration, Vibration control

Stefano Manzoni & Francescantonio Lucá
Department of Mechanical Engineering, Politecnico di Milano, Via La Masa, 1 - 20156 Milan, Italy
e-mail: stefano.manzoni@polimi.it

Marta Berardengo
Department of Mechanical, Energy, Management and Transportation Engineering, Universitá degli Studi di Genova, Via all'Opera Pia, 15a - 16145 Genoa, Italy, e-mail: marta.berardengo@unige.it

ISSN:3078-543X. Published by Eccomas Proceedia.
Peer-review under responsibility of the organizing committee of SMART 2025.
doi: 10.7712/150125.13710.303003

1 INTRODUCTION

Tuned mass dampers (TMD) are widely used systems for lowering vibrations of primary systems. Even if they are very effective when their dynamics is properly tuned on the dynamics of the primary system, they suffer of possible mistuning which significantly worsens the attenuation performance. Mistuning can occur when, as an example, thermal shifts change the dynamics of either the primary system or the TMD (or both).

To avoid mistuning, different types of adaptive TMDs (ATMD) are proposed in the literature using many different possible approaches (e.g., [1, 2, 3, 4, 5]). Most of the ATMDs are such that they can change their eigenfrequency in order to recover tuning when needed.

Among the possible approaches for making TMDs adaptive, the use of smart materials is gaining more and more attention because of their advantageous features, such as lightweight ease of use, limited cost. Different examples are available in the literature using, e.g., shape memory alloys [6, 7, 8, 9], piezoelectric elements [10, 11, 12, 13, 14, 15, 16, 17, 18] and magneto-rheological elements [19, 20].

This paper will show that when a mechanical structure (named here host structure) is coupled to two (or more) elements made from any intelligent material, it is possible to tune the eigenfrequency of two (or more) modes of the host structure at the same time with a certain degree of independence, thus obtaining a multi-frequency (or multi-resonant) ATMD. Therefore, the ATMD is made from the host structure and the coupled elements of intelligent material. The basic requirement is that the considered intelligent material shows both direct and inverse effect so that it is possible to define the so called modal coupling factor k_i (where the subscript i indicates the coupling factor is related to the i-th mode) for all the modes of the structure. This k_i is a non-dimensional measure of the efficiency of the energy conversion between the intelligent material and the i-th mode of the structure and vice versa.

There exist different types of intelligent materials with a double effect, such as piezoelectric elements [21] and magnetostrictive elements [22]. Nevertheless, also other physical phenomena involving a double effect can be used, such as in the case of, e.g., electro-magnetic devices [23]. In all these cases, it is possible to define k_i thanks to the presence of the double effect and this feature makes all these cases fine for developing multi-frequency ATMDs. This paper will use as example the case of piezoelectric elements but, as evidenced in the paper, the key parameters are the k_i of two (or more) modes and, therefore, the discussion can be considered valid also for other intelligent materials.

The paper is structured as follows: Section 2 will explain how the multi-frequency ATMD can be developed and how its degree of independence in tuning different eigenfrequencies is obtained, while Section 3 presents the tests carried out on a set-up to show the effectiveness of the approach.

2 THE MULTI-FREQUENCY ATMD

A multi-frequency ATMD can be built using piezoelectric elements employing, as an example, a cantilever beam of, e.g., steel, and bonding two (or more) piezoelectric patches in

Table 1: Values used for simulations aimed at showing the effects of α_p and β_p on the r_i values.

$\lvert k_{i=1,p=1}\rvert$	$\lvert k_{i=1,p=2}\rvert$	$\lvert k_{i=2,p=1}\rvert$	$\lvert k_{i=2,p=2}\rvert$	$C_{i=1,p=1}$ [nF]	$C_{i=1,p=2}$ [nF]	$C_{\infty,p=1}$ [nF]	$C_{\infty,p=2}$ [nF]
0.244	0.096	0.072	0.184	79.82	83.66	57.03	58.71

different locations along the beam. In the discussion here, two patches will be used.

According to [24], the i-th eigenfrequency can be shifted from ω_i to $\omega_{i,\text{new}}$ by shunting two capacitances to the two patches, one for each patch. The capacitances can be either positive (i.e., physical capacitances) or negative (i.e., simulated by using circuits based on operational amplifiers [25] since they do not exist in nature as physical components). It is noticed that ω_i is the i-th eigenfrequency with both the patches short-circuited. The relation between ω_i and $\omega_{i,\text{new}}$ is [24]:

$$\omega_{i,\text{new}}^2 = \omega_i^2 \left[1 + \frac{k_{i,p=1}^2}{(C_{\text{a},p=1}/C_{i,p=1}) + 1} + \frac{k_{i,p=2}^2}{(C_{\text{a},p=2}/C_{i,p=2}) + 1}\right] \tag{1}$$

where the subscript p indicates either piezoelectric element 1 or 2, $C_{i,p}$ is the modal capacitance of the p-th patch at the i-th mode (see [26] for the way to estimate this quantity) and $C_{\text{a},p}$ is the capacitance shunted to the p-th patch. Equation (1) can be also rearranged to express $C_{\text{a},p}$ as function of $\omega_{i,\text{new}}$ [24].

It is noticed that the $|k_{i,p}|$ value can be estimated as [21]:

$$|k_{i,p}| = \sqrt{\frac{\hat{\omega}_{i,p}^2 - \omega_i^2}{\omega_i^2}} \tag{2}$$

where $\hat{\omega}_{i,p}$ is the i-th eigenfrequency with all the patches short-circuited, exception made for the p-th patch which is open-circuited.

Equation (1) evidences that, having two shunt capacitances, it is possible to set the value of two $\omega_{i,\text{new}}$ values. Using three patches, it will be thus possible to set the value of three eigenfrequencies, etc. Considering again the example of two patches, Eq. (1) also suggests that, to have good independence in moving the value of the two considered eigenfrequencies, the best choice is to have either $|k_{i=1,p=1}|$ and $|k_{i=2,p=2}|$ large, and $|k_{i=1,p=2}|$ and $|k_{i=2,p=1}|$ small, or $|k_{i=1,p=2}|$ and $|k_{i=2,p=1}|$ large, and $|k_{i=1,p=1}|$ and $|k_{i=2,p=2}|$ small.

When the shunt capacitances are positive, the system is always stable, while, when negative capacitances are employed, stability must be checked. Four different stable configurations (named conf1 to conf4) exist [24]:

1.
$$C_{\text{a},p=1} < -C_{0,p=1}, \quad C_{\text{a},p=2} < -C_{i=1,p=2}(1 + k_{i=1,p=2}^2 X_{i=1,p=1}) \tag{3}$$

2.
$$C_{\text{a},p=1} > -C_{\infty,p=1}, \quad C_{\text{a},p=2} > -C_{\infty,p=2} \tag{4}$$

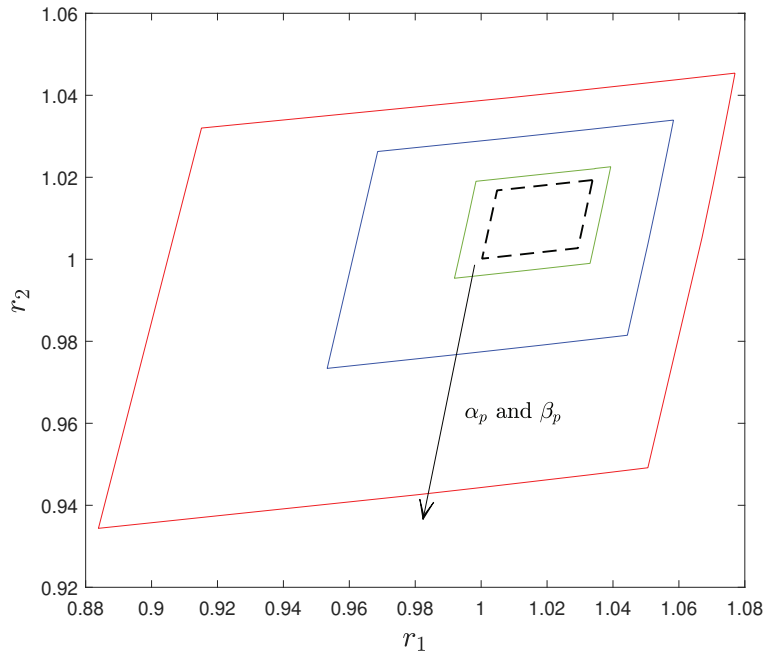


Figure 1: Resulting (r_1, r_2) areas (areas contained in the parallelograms) for different maximum values of α_p and β_p for the system of Table 1. Here, the maximum values for α_p and β_p are: 0.2, 0.6, 0.8 (solid lines in the plot). Furthermore, the case where only positive capacitances are used for shunting the two piezoelectric patches (i.e., $\beta_{p=1} \leq 0$ and $\beta_{p=2} \leq 0$) is also shown by means of a dashed line.

3.

$$C_{\mathrm{a},p=1} > -C_{\infty,p=1}, \quad C_{\mathrm{a},p=2} < -C_{0,p=2} \tag{5}$$

4.

$$C_{\mathrm{a},p=1} < -C_{0,p=1}, \quad C_{\mathrm{a},p=2} > -C_{\infty,p=2} \tag{6}$$

where:

$$X_{i=1,p=1} = \frac{C_{\mathrm{a},p=1} + C_{i=1,p=1}}{C_{\mathrm{a},p=1} + C_{0,p=1}} = \frac{C_{\mathrm{a},p=1} + C_{i=1,p=1}}{C_{\mathrm{a},p=1} + C_{i=1,p=1}(1 + k^2_{i=1,p=1})} \tag{7}$$

and $C_{0,p}$ is the value of the piezoelectric capacitance at the null frequency for the p-th piezoelectric patch ($C_{0,p} = C_{i=1,p}(1+k^2_{i=1,p})$ [25]). Finally, $C_{\infty,p}$ is the capacitance at constant strain for the p-th patch.

Defining:

$$\alpha_p = -C_{0,p}/C_{\mathrm{a},p}, \quad C_{\mathrm{a},p} < -C_{0,p} \tag{8}$$

$$\beta_p = C_{\mathrm{a},p}/(-C_{\infty,p}), \quad C_{\mathrm{a},p} > -C_{\infty,p} \tag{9}$$

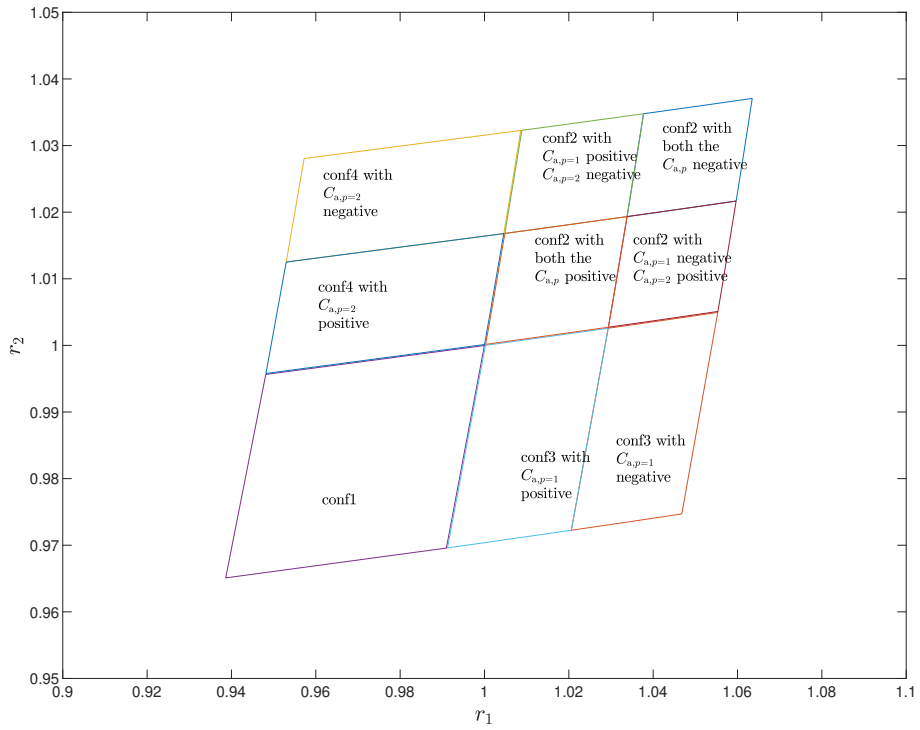


Figure 2: Resulting (r_1, r_2) areas (areas contained in the parallelograms) for different stable configurations of the shunt capacitances.

stability is assured when these two parameters are smaller than 1. Actually, when conf1 is used, according to Eq. (3), the actual stability limit is different from $-C_{0,p}$ for one of the two patches. However, for the sake of simplicity, here the stability limit is approximated to $-C_{0,p}$ for both the NCs connected to the patches.

The use of negative capacitances allows enlarging the achievable frequency changes. As an example, for a system having the features reported in Table 1, Fig. 1 shows that increasing the maximum possible value of α_p and β_p allows having wider and wider possible shifts of the two considered eigenfrequencies. In the figure, r_i expresses the following quantity:

$$r_i = \omega_{i,\text{new}}/\omega_i \tag{10}$$

Furthermore, Fig. 2 shows how the different shut configurations allows moving in different areas of the (r_1, r_2) plane.

The whole discussion can be replicated for other structures equipped, e.g., with electromagnetic devices or magnetostrictive elements, allowing to build ATMDs relying on different physical principles and intelligent materials. In these cases, the shunting elements would be

Table 2: Values of $|k_{i,p}|$, α_p and β_p for the tests. The values of $|k_{i,p}|$ were measured every time before each test for a better accuracy.

Test ID	$\lvert k_{i=1,p=1}\rvert$	$\lvert k_{i=1,p=2}\rvert$	$\lvert k_{i=2,p=1}\rvert$	$\lvert k_{i=2,p=2}\rvert$	$\alpha_{p=1}$ $\beta_{p=1}$	$\alpha_{p=2}$ $\beta_{p=2}$
T1	0.242	0.090	0.057	0.188	$\beta_{p=1}$=-1.14	$\alpha_{p=2}$=0.81
T2	0.242	0.094	0.066	0.186	$\beta_{p=1}$=0.69	$\alpha_{p=2}$=0.70
T3	0.242	0.094	0.071	0.184	$\beta_{p=1}$=0.45	$\beta_{p=2}$=0.57
T4	0.242	0.094	0.066	0.186	$\alpha_{p=1}$=0.66	$\alpha_{p=2}$=0.58

inductances.

3 EXPERIMENTS

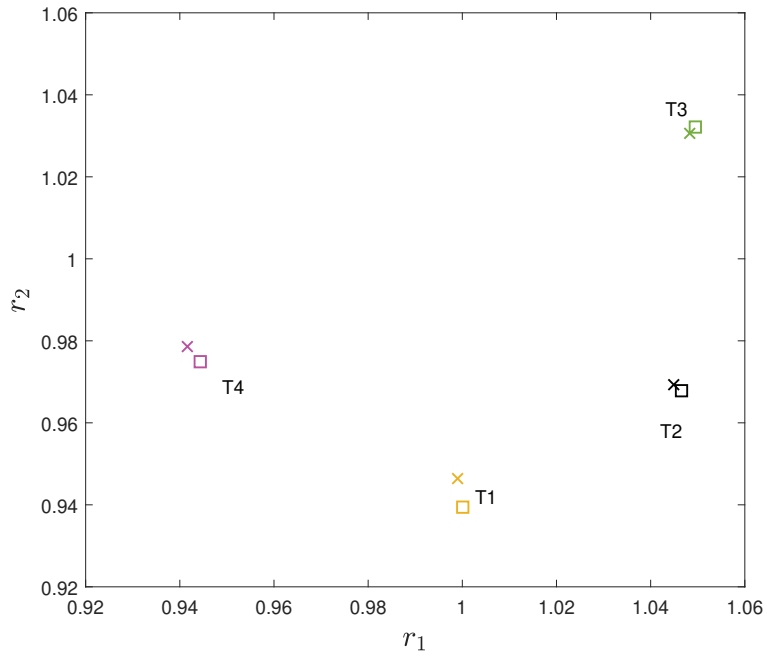


Figure 3: Experimental (x) and theoretical (□) results in terms of r_1 and r_2 values for the tests in Table 2.

In this section, few tests carried out on a cantilever beam equipped with two piezoelectric patches are discussed to show the reliability and feasibility of the proposed principle and treatment. The measured $\omega_i/(2\pi)$ of the first two bending modes of the beam were 22.2 and 124.5 Hz. Table 2 describes the tests considered here. Figure 3 shows that the theoretical expectation for the value of r_i is always close to the obtained experimental value. Many more tests and analyses are available in [24].

4 CONCLUSION

This paper has dealt with an approach for developing multi-frequency ATMDs able to shift two (or more) of its eigenfrequency with a given level of independence. This is obtained by using two (or more) elements made from intelligent material coupled to a mechanical system. The intelligent material used must show both direct and inverse effects.

Some experimental tests carried out on a cantilever beam equipped with two piezoelectric patches have confirmed that the approach is successful and good match was obtained with the theoretical expectations.

REFERENCES

[1] P. Gardonio, L. Ortis, E. Rustighi, C. Malacarne, and M. Perini, "Multi-resonant tva formed by a tree of deflated composite beams with core structured fabrics," *Smart Materials and Structures*, vol. 34, no. 1, 2025, 015039.

[2] P. Gardonio, E. Turco, A. Kras, L. Dal Bo, and D. E. Casagrande, "Semi-active vibration control unit tuned to maximise electric power dissipation," *Journal of Sound and Vibration*, vol. 499, 2021, 116000.

[3] L. Wang, S. Nagarajaiah, Y. Zhou, and W. Shi, "Experimental study on adaptive-passive tuned mass damper with variable stiffness for vertical human-induced vibration control," *Engineering Structures*, vol. 280, 2023, 115714.

[4] Z. H. Wang, Y. W. Xu, H. Gao, Z. Q. Chen, K. Xu, and S. B. Zhao, "Vibration control of a stay cable with a rotary electromagnetic inertial mass damper," *Smart Structures and Systems*, vol. 23, no. 6, p. 627 – 639, 2019.

[5] N. Carpineto, W. Lacarbonara, and F. Vestroni, "Hysteretic tuned mass dampers for structural vibration mitigation," *Journal of Sound and Vibration*, vol. 333, no. 5, p. 1302 – 1318, 2014.

[6] S. Manzoni, A. Argentino, F. Lucà, M. Berardengo, and M. Vanali, "Sma-based adaptive tuned mass dampers: Analysis and comparison," *Mechanical Systems and Signal Processing*, vol. 186, 2023, 109883.

[7] M. Berardengo, G. Della Porta, S. Manzoni, and M. Vanali, "A multi-modal adaptive tuned mass damper based on shape memory alloys," *Journal of Intelligent Material Systems and Structures*, vol. 30, no. 4, pp. 536–555, 2019.

[8] M. A. Savi, A. S. De Paula, and D. C. Lagoudas, "Numerical Investigation of an Adaptive Vibration Absorber Using Shape Memory Alloys," *Journal of Intelligent Material Systems and Structures*, vol. 22, no. 1, pp. 67–80, 2010.

[9] E. Rustighi, M. J. Brennan, and B. R. Mace, "A shape memory alloy adaptive tuned vibration absorber: design and implementation," *Smart Materials and Structures*, vol. 14, no. 1, pp. 19–28, 2005.

[10] G. M. Chatziathanasiou, N. A. Chrysochoidis, C. S. Rekatsinas, and D. A. Saravanos, "A semi-active shunted piezoelectric tuned-mass-damper for multi-modal vibration control of large flexible structures," *Journal of Sound and Vibration*, vol. 537, 2022, 117222.

[11] G. M. Chatziathanasiou, N. A. Chrysochoidis, and D. A. Saravanos, "A semi-active shunted piezoelectric tuned mass damper for robust vibration control," *Journal of Vibration and Control*, vol. 28, no. 21-22, p. 2969–2983, 2022.

[12] P. Gardonio, M. Zientek, and L. Dal Bo, "Panel with self-tuning shunted piezoelectric patches for broadband flexural vibration control," *Mechanical Systems and Signal Processing*, vol. 134, 2019, 106299.

[13] P. Gardonio, G. K. Rodrigues, L. Dal Bo, and E. Turco, "Extremum seeking online tuning of a piezoelectric vibration absorber based on the maximisation of the shunt electric power absorption," *Mechanical Systems and Signal Processing*, vol. 176, 2022, 109171.

[14] G. K. Rodrigues, P. Gardonio, L. Dal Bo, and E. Turco, "Piezoelectric patch vibration control unit connected to a self-tuning rl-shunt set to maximise electric power absorption," *Journal of Sound and Vibration*, vol. 536, 2022, 117154.

[15] D. E. Casagrande, P. Gardonio, and G. K. Rodrigues, "Tonal vibration control with a self-tuning absorber employing the extremum seeking algorithm," *Mechanical Systems and Signal Processing*, vol. 211, 2024, 111254.

[16] O. Heuss, R. Solloum, D. Mayer, and T. Melz, "Tuning of a vibration absorber with shunted piezoelectric transducers," *Archive of Applied Mechanics*, vol. 86, pp. 1715–1732, 2016.

[17] M. Lallart, L. Yan, Y.-C. Wu, and D. Guyomar, "Electromechanical semi-passive nonlinear tuned mass damper for efficient vibration damping," *Journal of Sound and Vibration*, vol. 332, no. 22, pp. 5696–5709, 2013.

[18] C. L. Davis and G. A. Lesieutre, "Actively tuned solid-state vibration absorber using capacitive shunting of piezoelectric stiffness," *Journal of Sound and Vibration*, vol. 232, no. 3, pp. 601–617, 2000.

[19] Y.-W. Xu, Z.-D. Xu, R.-L. Zhao, Z.-H. Wang, Y. Li, and C. Zhu, "Multimode vibration control of stay cables using pseudo negative stiffness mr damping system," *Journal of Intelligent Material Systems and Structures*, vol. 34, no. 14, p. 1617–1632, 2023.

[20] F. Weber, C. Boston, and M. Maślanka, "An adaptive tuned mass damper based on the emulation of positive and negative stiffness with an MR damper," *Smart Materials and Structures*, vol. 20, no. 1, 2011, 015012.

[21] O. Thomas, J. Ducarne, and J. De$\ddot{u}$, "Performance of piezoelectric shunts for vibration reduction," *Smart Materials and Structures*, vol. 21, no. 1, 2012, 015008.

[22] M. Berardengo, M. Mercato, and S. Manzoni, "Magnetostrictive shunt for vibration control and isolation: model, characteristics and similarities with piezoelectric shunt," *Smart Materials and Structures*, vol. 34, no. 1, 2025, 015043.

[23] M. Auleley, O. Thomas, C. Giraud-Audine, and H. Mahé, "Enhancement of a dynamic vibration absorber by means of an electromagnetic shunt," *Journal of Intelligent Material Systems and Structures*, vol. 32, no. 3, p. 331 – 354, 2021.

[24] S. Manzoni, M. Berardengo, F. Boccuto, and M. Vanali, "Piezoelectric-shunt-based approach for multi-mode adaptive tuned mass dampers," *Mechanical Systems and Signal Processing*, vol. 200, 2023, 110537.

[25] M. Berardengo, O. Thomas, C. Giraud-Audine, and S. Manzoni, "Improved resistive shunt by means of negative capacitance: new circuit, performances and multi mode control," *Smart Materials and Structures*, vol. 25, 2016, 075033.

[26] M. Berardengo, S. Manzoni, J. Høgsberg, and M. Vanali, "Vibration control with piezoelectric elements: The indirect measurement of the modal capacitance and coupling factor," *Mechanical Systems and Signal Processing*, vol. 151, 2021, 107350.